

## Effects of ionizing radiation in ceramics

R. Devanathan<sup>a,\*</sup>, K.E. Sickafus<sup>b</sup>, W.J. Weber<sup>a</sup>, M. Nastasi<sup>b</sup>

<sup>a</sup> Pacific Northwest National Laboratory, PO Box 999, MS K1-96, Richland, WA 99352, USA

<sup>b</sup> Los Alamos National Laboratory, Los Alamos, NM 87545, USA

### Abstract

The evolution of radiation damage in ceramics under highly ionizing conditions has been examined by irradiating a number of oxides with high-energy heavy ions and electrons simultaneously.  $\alpha$ -Al<sub>2</sub>O<sub>3</sub>, MgTiO<sub>3</sub>, FeTiO<sub>3</sub> and Ca<sub>2</sub>La<sub>8</sub>(SiO<sub>4</sub>)<sub>6</sub>O<sub>2</sub> were irradiated with 1 MeV Kr<sup>+</sup> or 1.5 MeV Xe<sup>+</sup> and 1 MeV electrons. The irradiations were performed in a high-voltage electron microscope interfaced to an ion accelerator that enabled the in situ observation of the structural changes. The results indicate that simultaneous electron irradiation can retard or prevent amorphization by heavy ions. Comparison with similar experiments in metals suggests that highly ionizing radiation can anneal damage to the crystal lattice in ceramics by enhancing the mobility of point defects. © 1998 Elsevier Science B.V.

### 1. Introduction

Ceramics have potential applications as low-activation structural and insulating materials in fusion reactors, electronic materials in radiation environments such as proposed space stations and actinide host phases in nuclear waste disposal. In all these applications, the material is likely to undergo displacement damage as well as ionization. Most of the previous studies of radiation damage in ceramics have focussed on displacement damage [1,2]. However, recent studies [3–10] have shown that ionization and energy transfers below the threshold for displacement damage can play an important role in the microstructural evolution of irradiated ceramics. It is, therefore, important to systematically examine the effects of ionization and sub-threshold events in a number of irradiated ceramics.

Some of the earliest studies of ionization effects in ceramics were performed by Krefft and co-workers [3,4] who found that ionizing radiation had an annealing effect on lattice damage in  $\alpha$ -Al<sub>2</sub>O<sub>3</sub> and MgO. The volumetric swelling induced by heavy-ion irradiation in these ionic materials was relieved by subsequent irradiation with 100 keV protons at room temperature. Based on these results, the authors have suggested that the charge state and mobil-

ity of the defects produced in ionic materials may depend on the fraction of the incident energy lost in electronic processes.

Bourgoin and Corbett [11] have reviewed mechanisms for the enhancement of defect migration by a change in the charge state of lattice defects. One of these, the Bourgoin mechanism, proposes the existence of defects in several charge states with the saddle point of one state coinciding with the energy minimum of another state and vice versa. An ionization-induced change in the charge state can cause a defect to go from an energy minimum to a saddle point. Relaxation to the minimum energy in the new state will lead to defect migration. Repeated changes of charge state can cause enhanced defect migration that can promote damage annealing in ionic materials. It must be pointed out that this mechanism is not efficient for long-range migration of defects. However, long-range migration might be enabled by the normal ionization-enhanced diffusion (IED) mechanism which proposes a large decrease in the migration energy of a point defect as a result of a change in charge state brought about by ionizing radiation. Other IED mechanisms, based on energy release from excited electronic states and rearrangement of bonds, have also been proposed [11].

Zinkle [5–7] has observed suppression of dislocation loop formation in periclase (MgO), spinel (MgAl<sub>2</sub>O<sub>4</sub>) and sapphire ( $\alpha$ -Al<sub>2</sub>O<sub>3</sub>) following light-ion (1 MeV H<sup>+</sup> or He<sup>+</sup>) irradiation at 923 K. The light ions produced larger

\* Corresponding author. Fax: +1-509 375 6631; e-mail: ram@pnl.gov.

loops with a much lower density compared to heavy ions. In addition, simultaneous irradiation of spinel with heavy (1.8 MeV  $\text{Cl}^+$  or 3.6 MeV  $\text{Fe}^+$ ) and light ions (1 MeV  $\text{He}^+$ ) was found to suppress loop nucleation when the light ion flux was sufficiently high. It was suggested that these effects are most likely due to ionization enhanced diffusion of point defects.

Recently, Devanathan et al. [8] have observed the suppression of heavy-ion induced amorphization of spinel at 100 K when the electronic stopping power was considerably higher than the nuclear stopping power. However, beam heating and chemical effects due to the implant may have played a role in these observations. It is, therefore, important to minimize chemical and beam heating effects, while studying the response of ceramics to highly ionizing radiation.

Simultaneous electron and heavy ion irradiation in a high-voltage electron microscope (HVEM) is one of the most convenient methods to study ionization effects in ceramics. The use of a HVEM enables the in situ observation of the state of damage in the material using electron microscopy and diffraction. In addition, the electron-transparent regions of the sample are too thin to retain a significant concentration of the implanting species. Furthermore, beam heating can be minimized by using a low flux of electrons and ions. Kinoshita et al. [9] have studied the effect of concurrent 30 keV  $\text{Xe}^+$  and 1 MeV electron irradiation on dislocation loop nucleation in spinel at 870 K. They did not observe the suppression of loop formation due to ionization seen by Zinkle [5–7]. This may be due to the fact that the 1 MeV electrons used by Kinoshita et al. produce homogeneous ionization as opposed to the highly localized ionization produced by the light ions in Zinkle's study. In addition, the 30 keV ions in Kinoshita's study were implanted into the specimen and may have assisted loop nucleation. The role of this homogeneous ionization in ceramics warrants further study, especially, under conditions where chemical effects are minimized.

Most of the previous studies of ionization effects in ceramics have been performed at elevated temperatures where radiation-induced phase transformations do not occur. Abe et al. [10] have examined the effect of concurrent electron irradiation on the heavy-ion induced amorphization of Si at room temperature. They found that electron irradiation resulted in retardation of ion-induced amorphization of Si. The authors have attributed this effect to athermal migration of point defects by energy transfers below the threshold displacement energy and atomic rearrangement due to electronic excitation.

In the present work, a number of ionic materials have been irradiated simultaneously with heavy-ions and electrons in a HVEM at temperatures as low as 26 K. The objective of the work is to examine the effect of simultaneous electron irradiation on the amorphization of ceramics brought about by heavy ion irradiation at cryogenic temperatures.

## 2. Experimental details

Single crystals of sapphire ( $\alpha\text{-Al}_2\text{O}_3$ ), geikielite ( $\text{MgTiO}_3$ ) and ilmenite ( $\text{FeTiO}_3$ ) were irradiated with 1 MeV  $\text{Kr}^+$  and 900 keV electrons. In addition, single crystals of apatite ( $\text{Ca}_2\text{La}_8(\text{SiO}_4)_6\text{O}_2$ ) were irradiated with 1.5 MeV  $\text{Xe}^+$  and 300 keV electrons. The samples were prepared by mechanical polishing using a tripod polisher [12] to achieve a thickness of less than 10  $\mu\text{m}$  and ion milling at room temperature with 5 keV Ar ions at 8° to the sample surface. The samples were not annealed following ion milling. The in situ irradiations were performed in the HVEM-Tandem Facility at Argonne National Laboratory, in which a 1.2 MeV modified Kratos/AEI EM7 electron microscope is interfaced to two National Electrostatics Corporation ion accelerators [13].

Liquid helium was used to cool the double-tilt sample holder to temperatures as low as 20 K during the irradiation. The flux of ions was about  $1 \times 10^{12}$  ion/ $\text{cm}^2$  s, which corresponds to a maximum power of 0.24 W/ $\text{cm}^2$ . At this low power, ion-beam heating effects are not expected to be significant. The peak electron beam flux was about  $2 \times 10^{19}$  e $^-$ / $\text{cm}^2$  s, and the rates of peak electron and ion beam displacements per atom (dpa) were about  $5 \times 10^{-4}$  dpa/s. Electron dosimetry was performed using a Faraday cup located above the upper objective pole piece and another located below the third projector lens. The electron dpa was estimated from Oen's tables [14], while the ion dpa was determined using TRIM 96 [15] calculations. An average displacement threshold energy of 40 eV was used.

The experimental setup used for dual-beam irradiation of  $\alpha\text{-Al}_2\text{O}_3$ ,  $\text{MgTiO}_3$  and  $\text{FeTiO}_3$  is schematically illustrated in Fig. 1. The ion beam irradiates the whole sample with a uniform flux, while the focussed electron beam has a Gaussian flux profile [13] with a half-width at half maximum of about 2  $\mu\text{m}$ . According to TRIM 96 [15] calculations, the ratio of electronic to nuclear stopping power,  $S_e/S_n$ , for 1 MeV  $\text{Kr}^+$  irradiation of a 50 nm thick sample of sapphire is about 1.15 at the top surface and 1 at the exit surface. The corresponding values for 1.5 MeV  $\text{Xe}^+$  are about 0.68 and 0.6. For the electron beam, the nuclear stopping power above and below the threshold for displacement was calculated using the McKinley-Feshbach approximation [16]. The integral was evaluated between 40 eV and the maximum transferred energy for nuclear stopping above the threshold. For sub-threshold nuclear stopping, the limits of integration were set at 0.1 and 40 eV. The electronic stopping power was determined using the Bethe-Bloch theory [17,18] for relativistic electrons.

Due to the Gaussian shape of the electron beam, the stopping power ratio varies as a function of radius of the electron beam for dual-beam irradiations.  $S_e/S_n$  at the center of the electron beam is about  $1 \times 10^4$ , four orders of magnitude higher than that at a distance of 5  $\mu\text{m}$  from

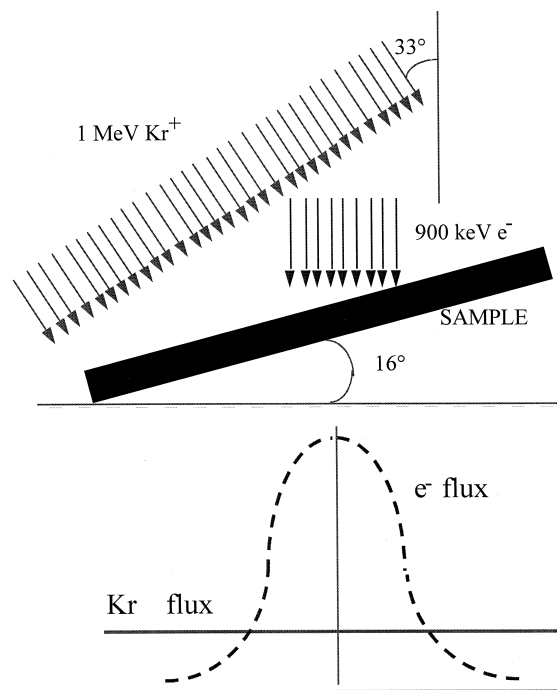


Fig. 1. Schematic diagram of the dual beam irradiation experiments.

the center where the sample is irradiated predominantly by ions. The calculated stopping power ratio for dual-beam irradiation of sapphire is shown in Fig. 2. The microstructure inside the electron beam was compared to that outside, to study the influence of a homogeneously ionizing radiation on the materials. For the apatite sample, a fully focussed electron beam was not used. In this case, the dose for amorphization by heavy ions was determined with the electron beam focussed to a radius of about 10 μm, and

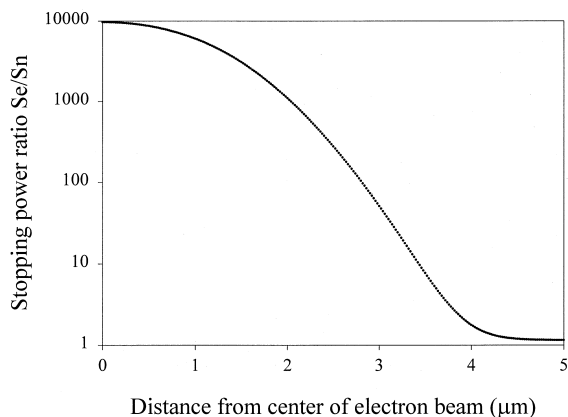


Fig. 2. The ratio of electronic to nuclear stopping power for simultaneous 1 MeV Kr<sup>+</sup> and 900 keV electron irradiation of sapphire.

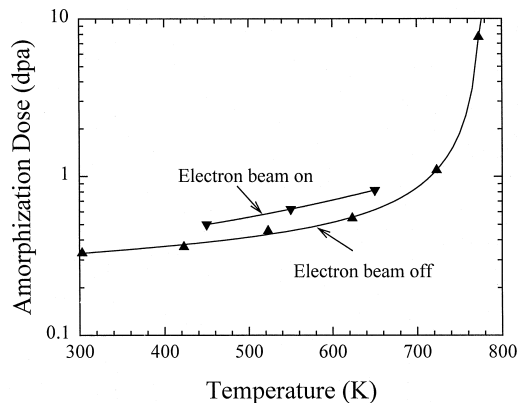


Fig. 3. The critical dose for amorphization of apatite by 1.5 MeV Xe<sup>+</sup> with and without a 300 keV electron beam.

also with the electron beam completely defocused (effectively off).

### 3. Results

Fig. 3 shows the amorphization dose in dpa for apatite (Ca<sub>2</sub>La<sub>8</sub>(SiO<sub>4</sub>)<sub>6</sub>O<sub>2</sub>) irradiated with 1.5 MeV Xe<sup>+</sup> as a function of temperature with and without a 300 keV electron beam. In the presence of the electron beam focussed to a radius of about 10 μm, the amorphization dose was found to be about 30% higher than with the electron beam off. This effect is significant in light of the fact that the electron beam was not fully focussed on a small area. When a fully focussed, 900 keV electron beam was used to irradiate three rhombohedral oxides, FeTiO<sub>3</sub>, MgTiO<sub>3</sub> and α-Al<sub>2</sub>O<sub>3</sub>, the retardation of amorphization was considerable.

Table 1 lists the displacement dose in dpa for amorphization of FeTiO<sub>3</sub> following irradiation by 1 MeV Kr<sup>+</sup> ions, and a simultaneous irradiation using a focussed 900 keV electron beam and 1 MeV Kr<sup>+</sup> ions. The amorphization dose for dual beam irradiation is more than twice that for the ion irradiation. In addition, the critical temperature for amorphization by dual beams is lower than that for amor-

Table 1  
Critical dose for amorphization of FeTiO<sub>3</sub> by 1 MeV Kr<sup>+</sup> ions and dual beams of 1 MeV Kr<sup>+</sup> and 900 keV electrons. C indicates that the material remains crystalline

Temperature (K)	Ion dose (dpa)	Dual beam dose (dpa)
30	0.19	0.40
100	0.23	0.47
150	0.38	3.10
175	1.13	4.50
200	2.25	C
300	C	C

Table 2  
Critical dose for amorphization of  $\text{MgTiO}_3$  by 1 MeV  $\text{Kr}^+$  ions and dual beams of 1 MeV  $\text{Kr}^+$  and 900 keV electrons

Temperature (K)	Ion dose (dpa)	Dual beam dose (dpa)
28	0.80	2.20
100	2.00	4.50
120	3.65	C
150	C	C

phization by 1 MeV  $\text{Kr}^+$ . Irradiation of  $\text{FeTiO}_3$  with a focussed beam of 900 keV electrons at 30 K, without the presence of ions, did not produce amorphization after 6

dpa. The dose for amorphization by heavy ions at this temperature is about 0.2 dpa.

A similar retarding effect due to simultaneous 900 keV electron irradiation was observed during 1 MeV  $\text{Kr}^+$  irradiation of  $\text{MgTiO}_3$  and these results are listed in Table 2. The areas inside the electron beam require much higher doses to go amorphous and have a lower critical temperature for amorphization. In both Tables 1 and 2, a C is used to denote that the material remained crystalline. At these temperatures, point defect clusters were observed indicating considerable defect mobility.

Fig. 4(a–c) are diffraction patterns and 4d is a bright-field (BF) image from an area of a sapphire sample

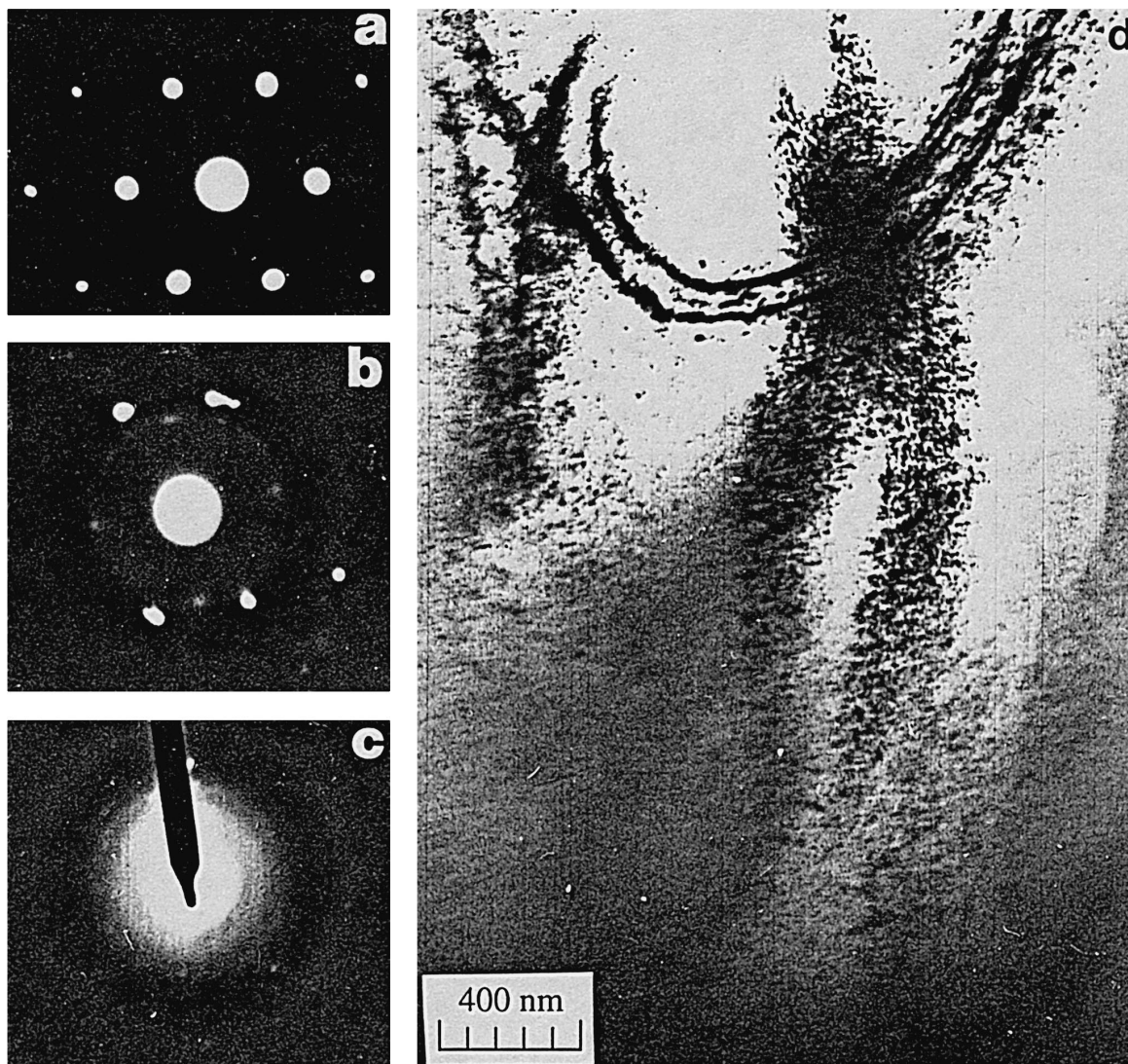


Fig. 4. Sapphire irradiated with 1 MeV  $\text{Kr}^+$  and 900 keV  $e^-$  at 26 K. Diffraction patterns from the region (a) at the center of the focussed  $e^-$  beam; (b) at the edge of the  $e^-$  beam and (c) irradiated predominantly with  $\text{Kr}^+$ . (d) Bright-field image showing the dual-beam irradiated region.

irradiated with both 900 keV focused electrons (2.3 peak dpa) and 1 MeV Kr<sup>+</sup> (3 dpa) at about 26 K. The electron diffraction pattern from the region at the center of the focussed electron beam (Fig. 4a) shows a perfectly crystalline spot pattern. The area at the edge of the electron beam shows a ‘spots and halo’ pattern (Fig. 4b). A completely amorphous halo pattern (Fig. 4c) is obtained far away from the electron irradiated region. The BF image (Fig. 4d) shows that the center of the electron irradiated region stays crystalline with uninterrupted bend contours and a high concentration of point defect clusters. This indicates that the region is crystalline and point defects are mobile. Moving towards the areas irradiated predominantly with Kr<sup>+</sup>, the bend contours gradually disappear indicating a transformation to the amorphous state.

The minimum ratio of electron to ion dpa rates ( $D_e/D_i$ ) needed to retard amorphization can be determined from the flux profile of the electrons and the distance from the center of the electron beam at which the bend contour disappears. We have determined this ratio to be 0.05 in  $\alpha$ -Al<sub>2</sub>O<sub>3</sub> at 26 K. The thermal conductivity of unirradiated  $\alpha$ -Al<sub>2</sub>O<sub>3</sub> is about 6000 W/mK at this temperature [19]. Point defects produced by radiation will cause a degradation in thermal conductivity. In spite of this degradation, beam heating is likely to be negligible and cannot be considered the cause for the observed suppression of ion beam induced amorphization [20]. The retention of crystallinity in the electron irradiated region at 26 K up to a dose of about 5 dpa is quite remarkable in light of the fact that sapphire can be readily amorphized by heavy ions at this dose above 100 K [21].

#### 4. Discussion

The retardation or suppression of heavy-ion induced amorphization by simultaneous electron irradiation observed in sapphire, ilmenite, geikielite and apatite in the present work is similar to that previously documented in metals. Koike [22] irradiated CuTi with 1 MeV electrons and 1 MeV Kr<sup>+</sup> at several temperatures. The critical temperatures for amorphization by 1 MeV electrons ( $T_c^e$ ) and 1 MeV Kr<sup>+</sup> ( $T_c^i$ ) were found to be 220 and 460 K, respectively. Below  $T_c^e$ , the dual-beam irradiated region went amorphous before the ion irradiated region. In contrast, above  $T_c^e$ , the electron irradiation retarded ion beam induced amorphization.

Koike [22] has pointed out that the excess vacancies created by electron irradiation are immobile below  $T_c^e$  and augment the displacement damage. Above  $T_c^e$ , they become mobile and anneal the damage created by the ion beam. This type of diffusion is known as radiation-enhanced diffusion. The irradiation of sapphire by 900 keV electrons will give rise to a non-equilibrium concentration of point defects. However, this excess alone cannot explain the present observations. For instance, the minimum  $D_e/D_i$  needed to retard amorphization in CuTi was determined by

Koike [22] to be 6, which is much higher than the value of 0.05 for sapphire in the present work. At a value of 0.05, the electron damage rate is too low to account for the suppression of amorphization. Moreover, the irradiation of sapphire was performed at a considerably lower temperature (26 K) compared to that of CuTi (300 K). According to the diffusion data available for Al<sub>2</sub>O<sub>3</sub> [23], the point defects would not be expected to migrate thermally during the experiment at 26 K. This suggests that the electron beam is much more effective in retarding amorphization in ceramics compared to metals and points to an athermal mechanism.

There are two athermal mechanisms that can be invoked to explain the observed retardation of amorphization, namely, sub-threshold energy transfer and ionization-enhanced diffusion. According to the sub-threshold model, pre-existing defects can migrate when an electron transfers energy less than the threshold for atomic displacement [10,24]. For instance, a transfer of about 2 eV to a point defect can cause it to make one diffusion jump. While this mechanism can cause local atomic rearrangement within cascades, it cannot lead to long-range diffusion.

Fig. 5 is a plot of the sub- and super-threshold nuclear and electronic stopping powers for high-energy electrons in sapphire. The general trends seen in this plot are true for all the ceramics studied in the present work. The electronic stopping power is nearly five orders of magnitude higher than the sub-threshold stopping power for 900 keV electrons. This arises from the fact that the cross-section, and hence the probability that an electron will lose a certain amount of energy, is orders of magnitude higher for electronic energy loss than for sub-threshold events. Thus, the observed retardation of amorphization is much more likely to arise from ionization-enhanced diffusion than from sub-threshold energy transfer.

The above argument in favor of ionization is supported by previous work. Ravi et al. [25] have shown that in situ

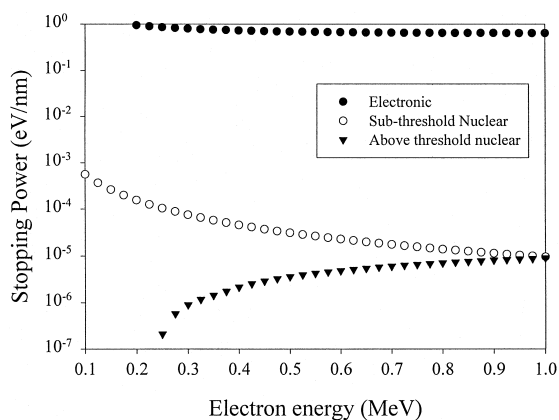


Fig. 5. The electronic, sub-threshold nuclear and above-threshold nuclear stopping powers for electrons in sapphire.

UV illumination during 150 keV self-ion implantation of Si samples cooled with liquid nitrogen leads to a significant suppression of radiation damage. The authors have suggested that enhanced defect migration due to a change in charge state of point defects could account for their observations. Jencic et al. [26] found that solid-phase epitaxial regrowth of spatially isolated amorphous regions in Si, Ge and GaP can be stimulated by 50 keV electron irradiation at room temperature. Their results indicate that electronic energy loss processes are responsible for the formation and migration of point defects.

The present observations in sapphire along with those in ilmenite, giekeilite and apatite are best explained by the mechanism of ionization enhanced diffusion. Electron irradiation of ceramics not only produces an excess of point defects, but also enhances their migration by ionization [27,28]. The resulting mobile defects help in annealing the damage to the lattice even at cryogenic temperatures as shown by the observation of point defect clusters in electron irradiated sapphire at 26 K. Retardation of amorphization also occurs at cryogenic temperatures in ilmenite and geikielite. In fact, ilmenite cannot be amorphized by electron irradiation at 30 K, even though it readily amorphizes under ion irradiation. In apatite, electron irradiation retards amorphization even under normal HVEM imaging conditions. Since the electron beam was not fully focused, the displacement rate was estimated to be of the order of  $10^{-6}$  dpa/s. This rate is too low to retard amorphization by radiation-enhanced diffusion.

The results from the present work are consistent with those of Zinkle [29] who found a strong correlation between point defect diffusion and large values of the electronic to nuclear stopping power ratio in irradiated ceramics. Zinkle also observed that point defect diffusion was enhanced in regions where the displacement damage rate was low, such as, the near-surface and mid-range regions in light-ion irradiated samples.

The present study has clearly demonstrated that electron irradiation can have a much more pronounced effect in ceramics compared to metals. In ceramics, electron irradiation at cryogenic temperatures does not simulate the conditions expected in a fusion reactor environment. However, it may be representative of radiation damage sustained by space stations and vehicles used for planetary exploration. Due to the presence of electrically charged defects in ionic materials, highly ionizing radiation can have an effect on microstructural evolution that is different from that in metallic materials. Therefore, damage accumulation models developed for irradiated metals cannot be directly extended to ceramics.

## 5. Summary

The effect of simultaneous electron and heavy-ion irradiation on the structure of  $\alpha$ -Al<sub>2</sub>O<sub>3</sub>, MgTiO<sub>3</sub>, FeTiO<sub>3</sub>,

and Ca<sub>2</sub>La<sub>3</sub>(SiO<sub>4</sub>)<sub>6</sub>O<sub>2</sub> has been examined in situ using a high voltage electron microscope. In all the compounds studied, electron irradiation was able to suppress or retard ion beam induced amorphization. In sapphire irradiated with dual beams at 26 K, point defect clusters formed and the material remained crystalline. The results indicate that highly ionizing radiation can enhance the mobility of point defects and anneal lattice damage even at cryogenic temperatures. The magnitude of this enhanced diffusion is significantly larger in ceramics compared to metals. Further work is needed to fully understand the effects of ionizing radiation in ceramics.

## Acknowledgements

This work is sponsored by the US Department of Energy, Division of Materials Sciences, Office of Basic Energy Sciences under Contract DE-AC06-76RLO 1830. One of the authors (R.D.) was supported by Associated Western Universities, Inc. under Grant DE-FG07-93ER-75912 with the US DOE. The authors are grateful to Edward A. Ryan, Stanley T. Ockers, Peter M. Baldo and Loren L. Funk of the HVEM-Tandem Facility at Argonne National Laboratory for their kind assistance with the irradiations.

## References

- [1] L.W. Hobbs, F.W. Clinard Jr., S.J. Zinkle, R.C. Ewing, *J. Nucl. Mater.* 216 (1994) 291.
- [2] R.C. Ewing, W.J. Weber, F.W. Clinard Jr., *Progr. Nucl. Energy* 29 (2) (1995) 63.
- [3] G.B. Krefft, *J. Vac. Sci. Technol.* 14 (1) (1977) 533.
- [4] G.W. Arnold, G.B. Krefft, C.B. Norris, *Appl. Phys. Lett.* 25 (1974) 540.
- [5] S.J. Zinkle, *Nucl. Instrum. Meth. B* 91 (1994) 234.
- [6] S.J. Zinkle, *J. Nucl. Mater.* 219 (1995) 113.
- [7] S.J. Zinkle, *Mater. Res. Soc. Symp. Proc.* 439 (1997) 667.
- [8] R. Devanathan, N. Yu, K.E. Sickafus, M. Nastasi, *Nucl. Instrum. Meth. B* 127&128 (1997) 608.
- [9] C. Kinoshita, H. Abe, S. Maeda, K. Fukumoto, *J. Nucl. Mater.* 219 (1995) 152.
- [10] H. Abe, C. Kinoshita, P.R. Okamoto, L.E. Rehn, *J. Nucl. Mater.* 212-215 (1994) 298.
- [11] J.C. Bourgoin, J.W. Corbett, *Radiat. Eff.* 36 (1978) 157.
- [12] J. Benedict, R. Anderson, S.J. Klepeis, *Mater. Res. Soc. Symp. Proc.* 254 (1991) 121.
- [13] C.W. Allen, L.L. Funk, E.A. Ryan, A. Taylor, *Nucl. Instrum. Meth. B* 40&41 (1988) 553.
- [14] O.S. Oen, U.S. Atomic Energy Commission Report, ORNL-4897, 1973.
- [15] J.F. Ziegler, J.P. Biersack, U. Littmark, *The Stopping and Range of Ions in Solids*, Pergamon, Oxford, 1985.
- [16] W.A. McKinley, H. Feshbach, *Phys. Rev.* 74 (1948) 1759.
- [17] H.A. Bethe, *Ann. Phys.* 5 (1930) 325.

- [18] H.A. Bethe, *Z. Phys.* 76 (1931) 293.
- [19] D. Strom, G. Wilham, P. Saunders, F.P. Lipschultz, in: P.G. Klemens, T.K. Chu (Eds.), *Thermal Conductivity*, vol. 14, Plenum, New York, 1976, p. 19.
- [20] I. Jencic, M.W. Bench, I.M. Robertson, M.A. Kirk, *J. Appl. Phys.* 78 (1995) 974.
- [21] H. Abe, S. Yamamoto, H. Naramoto, *Nucl. Instrum. Meth. B* 127&128 (1997) 170.
- [22] J. Koike, PhD thesis, Northwestern University, 1989, p. 118.
- [23] K.P.D. Lagerlof, T.E. Mitchell, A.H. Heuer, *J. Am. Ceram. Soc.* 72 (1989) 2159.
- [24] H. Abe, C. Kinoshita, Y. Denda, *Mater. Res. Soc. Symp. Proc.* 373 (1995) 487.
- [25] J. Ravi, Y. Erokhin, K. Christensen, G.A. Rozgonyi, B.K. Patnaik, C.W. White, *Mater. Res. Soc. Symp. Proc.* 373 (1995) 475.
- [26] I. Jencic, M.W. Bench, I.M. Robertson, M.A. Kirk, *Mater. Res. Soc. Symp. Proc.* 373 (1995) 481.
- [27] Y. Chen, M.M. Abraham, H.T. Tohver, *Phys. Rev. Lett.* 37 (1976) 1757.
- [28] S. Clement, E.R. Hodgson, *Phys. Rev. B* 36 (1987) 3359.
- [29] S.J. Zinkle, *Mater. Res. Soc. Symp. Proc.* 373 (1995) 287.